

MEDEA: A Design-Time Multi-Objective Manager for Energy-Efficient DNN Inference on Heterogeneous Ultra-Low Power Platforms

HOSSEIN TAJI, Embedded Systems Laboratory (ESL), EPFL, Switzerland

JOSÉ MIRANDA, Industrial Electronics Center (CEI), UPM, Spain

MIGUEL PEÓN-QUIRÓS, EcoCloud, EPFL, Switzerland

DAVID ATIENZA, Embedded Systems Laboratory (ESL), EPFL, Switzerland

The growing demand for on-device AI necessitates energy-efficient execution of DNN based applications on resource-constrained ultra-low power (ULP) platforms. Heterogeneous architectures, combining specialized processing elements (PEs), have emerged as a key solution for achieving the required performance and energy efficiency. However, optimizing energy while executing applications on these platforms requires efficiently managing platform resources like PEs, power features, and memory footprint, all while adhering to critical application deadlines. This paper presents MEDEA, a novel design-time multi-objective manager for energy-efficient DNN inference on Heterogeneous ULP (HULP) platforms. MEDEA uniquely integrates: kernel-level dynamic voltage and frequency scaling (DVFS) for dynamic energy adaptation; kernel-level granularity scheduling, suitable for specialized accelerators; memory-aware adaptive tiling to navigate severe memory constraints; and all within a timing constraint-based optimization strategy, which minimizes energy based on application deadline. To showcase practical viability, we evaluate MEDEA on HEEptimize, a heterogeneous ULP platform (22 nm, FPGA-prototyped) featuring a RISC-V processor besides Near-Memory Computing (NMC) and Coarse-Grained Reconfigurable Array (CGRA) accelerators. Experimental results, using a biomedical seizure detection case study, demonstrate that MEDEA achieves overall energy reductions of up to 38 % compared to representative state-of-the-art methods, while consistently meeting all timing and memory requirements. This effectiveness is attributed to its integrated features, with our analysis showing that kernel-level DVFS alone can be responsible for over 31 % of the energy savings in specific scenarios.

CCS Concepts: • **Computer systems organization** → **Embedded systems; Real-time systems; Heterogeneous (hybrid) systems;**
• **Hardware** → **Power and energy.**

Additional Key Words and Phrases: Ultra-Low Power (ULP) systems, DNN Inference Scheduling, Heterogeneous Multi-Accelerator Platforms, Runtime DVFS, Tiling, Energy Optimization.

1 Introduction

The increasing prevalence of AI, particularly DNN, is driving a shift towards the deployment of AI processing at the edge, closer to the data source. This paradigm offers compelling advantages over traditional cloud-based AI, including reduced latency, enhanced data privacy, lower bandwidth consumption, and offline operations capabilities [25, 28, 31]. However, executing computationally demanding DNNs on resource-constrained edge devices presents significant challenges, especially with respect to power and memory. To address these, *heterogeneous architectures* have emerged as a key solution [20]. By combining heterogeneous PEs (e.g., CPUs, specialized accelerators), architectural specialization allows significant improvements in both performance and energy efficiency compared to traditional homogeneous systems [24].

However, merely incorporating heterogeneous PEs is insufficient; Realizing the performance and energy benefits of heterogeneity depends on *effective resource management and scheduling* [13]. This involves intelligently assigning DNN computational tasks to the most suitable PEs [6, 12, 13, 26], dynamically adjusting operating points (such as

Authors' Contact Information: [Hossein Taji](mailto:Hossein.Taji@epfl.ch), hossein.taji@epfl.ch, Embedded Systems Laboratory (ESL), EPFL, Lausanne, Switzerland; [José Miranda](mailto:jose.miranda@upm.es), jose.miranda@upm.es, Industrial Electronics Center (CEI), UPM, Madrid, Spain; [Miguel Peón-Quirós](mailto:Miguel.Peon-Quiros@epfl.ch), miguel.peon@epfl.ch, EcoCloud, EPFL, Lausanne, Switzerland; [David Atienza](mailto:david.atienza@epfl.ch), david.atienza@epfl.ch, Embedded Systems Laboratory (ESL), EPFL, Lausanne, Switzerland.

voltage and frequency) through DVFS [16, 38], and efficiently handling data movement [3, 11, 32], while adhering to the application timing requirements [13, 37] and the limitations of the platform resources [25, 28, 31]. The challenge of resource management and scheduling becomes particularly acute in the *ULP* domain, where platforms operate under exceptionally stringent constraints, often characterized by mW or μ W power budgets and only KiB to MiB of available on-chip memory [25, 28, 31]. These severe limitations sharply distinguish ULP devices from the broader edge category, which includes significantly more capable platforms like mobile SoCs (e.g., [13, 14, 36]) or embedded systems such as the NVIDIA Jetson series (e.g., [2, 6, 12, 23]).

Particularly relevant to the ULP domain is the increasing adoption of the RISC-V Instruction Set Architecture (ISA), preferred for its open, modular, and extensible nature in resource-constrained embedded systems [20]. This trend has led to several heterogeneous ULP (HULP) platforms based on RISC-V explicitly designed for energy efficiency, such as DIANA [34], DARKSIDE [8], and HEEPocrates [19]. These platforms often integrate specialized hardware accelerators, crucial components of their heterogeneous design. Key paradigms include NMC units [4], which minimize costly data movement by computing near or within memory, and CGRAs [7], which offer a balance of hardware efficiency and software flexibility for diverse DNN kernels. These, among other specialized digital accelerators [8], are vital to efficiently execute demanding applications such as DNN-based ones on ULP platforms.

However, effective management and scheduling of DNNs on HULP platforms presents a unique confluence of challenges. Existing solutions [2, 3, 5, 6, 9, 10, 12–14, 17, 23, 26, 32, 35–37] often address certain aspects of edge deployment, but struggle to holistically tackle the combined demands inherent to the ULP domain. In fact, the main shortcomings, hindering optimal performance, include a lack of kernel-level DVFS, insufficient memory-aware adaptive tiling mechanisms for severe memory constraints, energy optimization frequently decoupled from strict application timing deadlines, coarse scheduling granularities are ill-suited for specialized accelerators, and often limited support beyond specific DNN architectures. To overcome these limitations, we propose **MEDEA** (**M**anager for **E**nergy-efficient **D**NNs on **h**eterogeneous **U**LP **A**rchitectures), a novel design-time multi-objective manager specifically designed for HULP platforms. Figure 1 presents an overview of MEDEA, illustrating how, based on DNN description, timing constraint, and platform characterization data, it generates per-kernel scheduling decisions determining the optimal PE, V-F setting, and tiling strategy for efficient execution on a HULP.

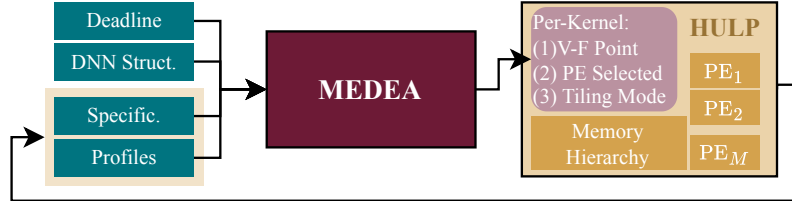


Fig. 1. Overview of the MEDEA design-time multi-objective manager, illustrating its kernel-level decisions on PE, V-F, and Tiling mode, used to orchestrate energy-efficient DNN inference on a HULP.

The main contributions of this paper are as follows:

- We introduce MEDEA, a novel design-time multi-objective manager tailored for HULPs. To the best of our knowledge, it is the first to integrate the following four features within a single, unified manager for HULPs: (1)

kernel-level DVFS for dynamic energy adaptation; (2) kernel-level scheduling granularity suitable for specialized accelerators; (3) memory-aware adaptive tiling to navigate severe memory constraints; all within a (4) timing constraint-based optimization strategy that minimizes energy based on application deadlines.

- We demonstrate the real-world applicability and effectiveness of MEDEA by applying it to a Transformer-based biomedical seizure detection application. Our evaluation includes a study on the impact of varying application deadlines on energy performance trade-offs and scheduling decisions made by MEDEA. This application study shows that our approach achieves energy reductions of up to 38 % compared to relevant baselines, while consistently meeting all timing requirements.
- We provide an in-depth analysis that isolates and quantifies the distinct energy savings enabled by MEDEA’s core features. Our evaluations demonstrate that, depending on the operational scenario and deadline, its kernel-level DVFS enables up to 31.3 % energy reduction, memory-aware adaptive tiling up to 8.5 %, and kernel-level scheduling up to 2.8 %, highlighting the individual importance of each integrated mechanism.

The remainder of this paper is organized as follows: Section 2 reviews state-of-the-art approaches on scheduling and energy optimization of DNN-based applications on heterogeneous platforms. Our proposed multi-objective manager, MEDEA, is detailed in Section 3. Section 4 describes the overall experimental setup. Section 5 presents and discusses the experimental results. Finally, Section 6 summarizes the main conclusions of this work.

2 Related Work

Table 1. Comparative Analysis of State-of-the-Art DNN Deployment and Optimization Approaches for Heterogeneous Platforms.

Approach	DVFS-Aware	Tiling-Aware	Deadline-Aware	Energy-Aware	DNN-Agnostic	Kernel-level Granul.
MATCH [9]	No	Yes	No	Yes(Trd.) ⁱ	No	Yes
RoaD-RuNNer [12]	No	No	No	Yes(Trd.)	No	No
AdaKnife [17]	Yes(App)	No ^a	No	No	Yes	No ^b
Kang et al. [13]	Yes(App)	No	Yes	Yes(Opt.) ⁱ	No	No
DORY [3]	No	Yes	No	No	No	N/A ^f
FDT [32]	No	Yes	No	No	No	N/A ^f
ODIMO [26]	No	N/S ^d	No	Yes(Trd.)	No	Yes
Wang et al. [36]	No	No	No	No	No	No
Vasiliadis et al. [35]	No	No	No	Yes(Trd.)	Yes	No
AxoNN [6]	No	No	No	Yes(Trd.)	No	No
Map-and-Conquer [2]	Yes(Layer)	No	Yes	Yes(Opt.)	Yes	No ^g
TensorRT (Jeong) [10]	No	No	No	No	No	No
DART [37]	No	No	Yes	No	No	No
HaX-CoNN [5]	No	No ^c	Yes	Yes(Trd.)	No	No
OmniBoost [14]	No	No	No	No	No	No
MaGNAS [23]	Yes(App)	No	Yes	Yes(Opt.)	No	No ^h
MEDEA (Ours)	Yes(Kernel)	Yes(Adap.)	Yes	Yes (Opt.)	Yes	Yes^e

^a Cannot tile kernels that individually exceed PE memory, although network partitioning respects PE limits. ^b Mixed granularity: Kernel/layer-level for CNNs; coarser (e.g., encoder block) for Transformers. ^c Manages shared memory contention/throughput, but not PE memory capacity limits. ^d Memory management details not specified, despite hardware-aware PE selection. ^e Supports any DNN composed of supported kernels (e.g., Conv, MatMul, FFT, Add, Norm); evaluated on Transformers. ^f Focuses only on tiling generation for specified DNN types, not full runtime execution management. ^g Partitions layers width-wise (e.g., CNN channels, Transformer heads) for mapping to CUs. ^h Scheduling occurs at the GNN block level (e.g., Grapher, FFN), specific to GNNs. ⁱ Trd.: Considers energy-speedup tradeoff. Opt.: Optimizes energy for a given deadline.

The efficient management of DNNs on heterogeneous edge platforms is an active and multifaceted research area. This review analyzes a wide range of state-of-the-art approaches to resource management to gain a comprehensive overview. It extends beyond end-to-end schedulers to include specialized optimization frameworks. We consider works focused primarily on ULP’s memory optimization through automated tiling (DORY [3], FDT [32]), and design-time compilation and training-time mapping for HULPs (MATCH [9], ODIMO [26]). Targetting edge, yet still resource-aware, platforms, we also examine runtime schedulers and partitioners targeting diverse objectives such as energy-latency tradeoffs (Kang et al. [13], AxoNN [6], Map-and-Conquer [2]), real-time guarantees (DART [37]), throughput maximization (TensorRT [10], OmniBoost [14], [36]), multi-DNN contention (HaX-CoNN [5]), and architecture-mapping co-design (MaGNAS [23]). Despite valuable contributions from these varied domains, our analysis reveals significant gaps in providing a holistic solution for HULPs, particularly concerning the integration of fine-grained, DVFS-, tiling-, and deadline-aware energy optimized manager. Table 1 provides a comparative summary, and the following paragraphs will analyze these key features in detail.

Scheduling Granularity and DNN Architecture Support. The effectiveness of a DNN manager on HULPs is largely determined by its scheduling granularity, the fundamental unit of work it manages. We define scheduling granularity by the size of the computational unit managed: a *layer* (e.g., a complete convolutional layer or Transformer block) is a high-level structural component, whereas a *kernel* (or operator, e.g., matrix multiplication, 2D convolution, an activation function) is a fundamental mathematical operation within such layers. We argue that a fine, kernel-level granularity is paramount on HULPs, as it not only allows for precise resource control but also provides inherent support for diverse DNN architectures, a feature lacking in many specialized, architecture-centric solutions. However, the one limitation of many existing approaches is their *architecture-centric design*. The majority of these frameworks are *CNN-centric* [5, 6, 9, 10, 12–14, 26, 36, 37], effectively making them specialized CNN managers rather than general DNN solutions. This specific focus is also apparent in other architecture-centric managers like MaGNAS [23] for GNNs. The other limitation is the *coarse scheduling granularity* of many existing approaches, often align with high-level structural components in comparison to individual kernels, such as entire inferences [35, 36] or a group of computations at different levels [2, 5, 6, 10, 13, 14, 17, 26, 37], for example, grouping such as width-wise splits of attention heads or channels [2, 26]. Thus, a significant gap remains for solutions that leverage deep kernel-level control to provide inherent unified support for diverse DNN architectures on HULP platforms.

DVFS and its Granularity. A key differentiator in energy-efficient resource management and scheduling is the utilization of DVFS, a fundamental power management technique that achieves significant energy savings by dynamically adjusting PE voltage and frequency to match the target workload, leveraging the quadratic power-voltage relationship ($P \propto V^2 f$) [16, 38]. While hardware platforms like Zero-riscy [22] and Raven [15] demonstrate its feasibility of runtime DVFS control in RISC-V based ULPs, our review reveals that existing approaches utilize this capability at varying levels of granularity, if at all. A significant majority of the analyzed related works do not incorporate any form of DVFS. This includes approaches focused on compilation (MATCH [9], DORY [3], FDT [32]), partitioning/offloading (RoAD-RuNNer [12]), training-time mapping (ODIMO [26]), runtime scheduling primarily for throughput or contention management (TensorRT-based [10], DART [37], HaX-CoNN [5], OmniBoost [14]), adaptive device selection [35], and energy-aware layer mapping [6]. Even works characterizing platform performance often neglect to detail DVFS utilization [36]. These approaches cannot dynamically adjust operating points to minimize energy based on the immediate needs of different DNN kernels, often defaulting to fixed performance settings. Several works consider DVFS, but typically at a coarse granularity throughout the application. For example, MaGNAS [23] selects a fixed V-F during its design-time search;

Kang et al. [13] account for the effects of V-F in its profiling; and AdaKnife [17] explores static frequency adjustments. Map-and-Conquer [2] incorporates DVFS as an optimization parameter in its coarse-layer granularity scheduling. This general absence of dynamic, fine-grained, kernel-level DVFS in the literature indicates a significant missed opportunity for energy savings on HULPs.

Tiling-Awareness for Constrained Memory. A few approaches, despite lacking other features, such as kernel-level DVFS scheduling or strict deadline-driven optimization, provide effective solutions specifically for tiling and memory management. For instance, DORY [3] uses constraint programming to optimize tiling for limited SRAM on PULP devices. FDT [32] introduces a specialized depthwise tiling method specifically for TinyML memory optimization. The MATCH [9] compilation framework employs Design Space Exploration (DSE) to determine effective tiling strategies based on HW models. However, many other approaches lack comprehensive memory awareness of individual PE capacity limits. Although some consider related aspects such as memory contention between concurrent DNNs (HaX-CoNN [5]), data transfer overheads ([2, 6, 13, 23, 35, 36]), or aim for reduced memory usage (AdaKnife [17]), they do not implement tiling specifically to fit operations exceeding PE memory capacity. Several other frameworks do not appear to incorporate PE memory constraints or tiling mechanisms at all (e.g., [10, 12, 14, 37]). With the exception of works mainly focused on tiling strategies or memory-centric compilation, many existing approaches do not deeply integrate robust, memory-aware tiling based on PE capacity into their core decision-making processes, representing a critical gap for practical deployment.

Deadline-Awareness and Energy Optimization. Effective resource management and scheduling for HULPs require simultaneously considering application time constraints (deadlines) and optimizing energy efficiency, often involving an explicit energy performance trade-off. Several works incorporate these aspects to varying degrees, though often with limitations in other critical areas like granularity or dynamic power management. Some approaches explicitly target both: Kang et al. [13] employ a GA-based scheduler that considers deadlines (via penalty) and allows users to select energy-latency trade-off points. Map-and-Conquer [2] includes target latency constraints and energy modeling. MaGNAS [23] co-optimizes GNN architecture and mapping under latency constraints while considering energy tradeoffs. HaX-CoNN [5] implicitly addresses timing via QoS requirements while considering PE power consumption. Other works prioritize meeting deadlines without deep energy optimization, such as DART [37] for real-time tasks. In contrast, several frameworks explore energy vs. performance trade-offs or specific energy targets but without strictly adhering to application deadlines. For instance, AxoNN [6] minimizes time under an energy budget, RoaD-RuNNer [12] finds Pareto optimal energy/latency points, and ODIMO [26] balances accuracy and efficiency. Frameworks like Vasiliadis et al. [35], MATCH [9], and the TensorRT-based approach [10] offer options to minimize energy or latency but lack a mechanism to enforce a strict timing constraint during optimization. Frameworks centered on memory optimization through tiling (e.g., DORY [3], FDT [32]), throughput maximization (e.g., OmniBoost [14]), or partitioning/offloading latency (e.g., AdaKnife [17]) often lack explicit mechanisms for managing energy consumption within a specific timing budget. Even works characterizing platform performance [36] typically do not go into deadline-driven scheduling.

Summary of Gaps and Proposed Approach. In summary, our review (Table 1) highlights several significant gaps in current resource management and scheduling approaches when applied to HULPs. These include a prevalent lack of kernel-level DVFS, insufficient memory-aware tiling, limited focus on optimizing energy under strict timing constraints, and coarse scheduling granularities unsuitable for specialized accelerators and restricted DNN architecture support. Collectively, these limitations hinder the ability to fully utilize the potential of HULP platforms for energy-efficient

execution of DNN-based applications. Although individual works may address some of these aspects, a holistic solution that effectively integrates all these demanding requirements for the ULP domain has been notably absent. To address this confluence of challenges, this paper proposes MEDEA, a novel design-time multi-objective manager that integrates kernel-level scheduling, kernel-level DVFS, memory-aware adaptive tiling within a flexible, timing-constrained energy optimization strategy explicitly tailored for HULPs.

3 MEDEA, Our Proposed Design-Time Multi-Objective Manager

This section details MEDEA, our proposed design-time multi-objective manager designed for energy-efficient, latency-constrained DNN inference on HULPs. Figure 2 provides a high-level overview of the MEDEA manager, illustrating its key inputs (application representation, platform characteristics, timing constraints), the control knobs it manipulates (PE assignment, V-F settings, tiling modes), and its core management and optimization algorithm. Each of these aspects will be described in detail in the following subsections.

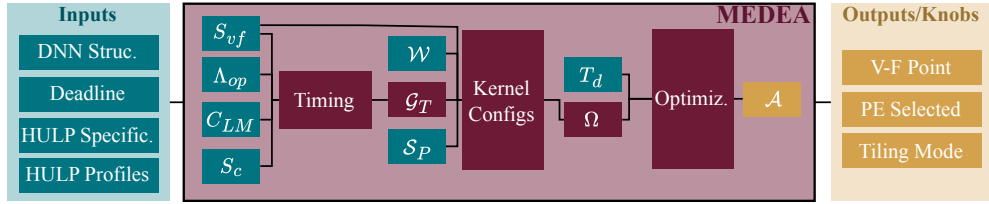


Fig. 2. Overview of the MEDEA design-time multi-objective manager, illustrating its inputs, output/knobs, and core management and optimization.

3.1 MEDEA Input Requirements

As illustrated in Figure 2, MEDEA relies on a set of inputs: (1) the DNN-based application structure to be scheduled, (2) its associated timing constraint, (3) HULP’s specifications, and (4) HULP’s performance profiles derived from characterization. The following subsections detail these required inputs.

3.1.1 Application Structure and Timing Constraint. MEDEA requires the workload structure and its timing constraint. First, the target DNN-based application structure is presented as a sequential workload \mathcal{W} , which is an ordered list of $N_{\mathcal{W}}$ computational kernels:

$$\mathcal{W} = \{k_1, k_2, \dots, k_{N_{\mathcal{W}}}\} \quad (1)$$

Each kernel k_i within this workload is defined by a tuple (τ_i, s_i, δ_i) , where $\tau_i \in \mathcal{T}_{ops}$ denotes the type of kernel, e.g., $\mathcal{T}_{ops} = \{\text{matmul}, \text{conv2d}, \text{norm}, \text{add}, \dots\}$; s_i represents its operational size or dimensions (e.g., matrix dimensions for matmul); and δ_i specifies the data width (e.g., int8, int16). This kernel-level representation is fundamental to the fine-grained optimization performed by MEDEA. Helper utilities are provided to aid in generating \mathcal{W} from higher-level descriptions (e.g., DNN model layers). Coarser-grained scheduling approaches, considered for comparison, typically group consecutive kernels from \mathcal{W} into larger blocks. The second input is the overall application timing constraint, or deadline T_d . This deadline dictates the maximum allowable active execution time for the entire workload \mathcal{W} and serves as the trade-off point for the energy optimization performed across the sequence of kernels.

3.1.2 *HULP's Specifications.* This begins with defining the set \mathcal{P} of $N_{\mathcal{P}}$ distinct PEs:

$$\mathcal{P} = \{p_1, p_2, \dots, p_{N_{\mathcal{P}}}\}. \quad (2)$$

Thus, \mathcal{P} typically includes one or more general-purpose CPUs (e.g., p_{cpu}) and various specialized accelerators (e.g., p_{acc1}). The platform operates across a discrete set \mathcal{V} of $N_{\mathcal{V}}$ voltage levels, with available V-F operating points forming a set S_{vf} :

$$S_{vf} = \{(v_l, f_l) \mid v_l \in \mathcal{V}, l = 1, \dots, N_{\mathcal{V}}\}, \quad (3)$$

where, consistent with common practice in works like [33], the system is usually operating at the maximum supported frequency, $f_l = F_{max}(v_l)$, at voltage v_l .

The platform's memory hierarchy is also important to know where data is available to be processed and how moving data between different levels should be handled. Beyond off-chip flash for global DNN weights, this can include a shared memory resource (e.g., L2 cache or main on-chip memory) with capacity C_M , and/or private local memories (LMs) for each PE $p_j \in \mathcal{P}$. PEs are assumed to operate primarily on data residing in their respective LMs. The set of all LM capacities is given by:

$$C_{LM} = \{(p_j, C_{LM_j}) \mid p_j \in \mathcal{P}\}. \quad (4)$$

Furthermore, MEDEA considers kernel-PE operational constraints, where each PE p_j may impose limitations on specific kernel types τ_i (e.g., maximum supported matrix dimensions for a matmul kernel). These specific constraint values are denoted as λ_{p_j, τ_i} , forming the set Λ_{op} :

$$\Lambda_{op} = \{(p_j, \tau_i, \lambda_{p_j, \tau_i}) \mid p_j \in \mathcal{P}, \tau_i \in \mathcal{T}_{ops}\}. \quad (5)$$

These specifications define the fixed capabilities and limitations of the hardware that MEDEA must operate within.

3.1.3 *HULP's Performance Profiles.* Additionally MEDEA utilizes dynamic performance profiles derived from representative kernel executions on the target platform. These profiles provide the performance metrics that form the basis for MEDEA's optimization process. First, *Timing Profiles* (S_c) detail measured cycle counts for representative kernels k_i (based on its operational size s_i and data width δ_i) on each relevant PE p_j . These profiles contain processing-only cycles and data movement characteristics that MEDEA utilizes alongside Λ_{op} and C_{LM_j} to estimate cycle counts for the different tiled execution modes (Sec. 3.2). Second, *Power Profiles* (S_p) supply characterized power information for each kernel k_i executing on PE p_j across different voltage levels v_l . This includes separated static (P_{stat}) and dynamic (P_{dyn_base} at a reference frequency f_{base}) power components. A common technique to decouple these components involves measuring at least in two different frequencies for a given voltage [20]. Lastly, the global idle / sleep power of the platform, P_{slp} , must also be profiled and provided.

3.2 MEDEA Outputs/Knobs

Figure 2 illustrates the outputs or control knobs that MEDEA manipulates to generate an energy-efficient, per-kernel decisions (\mathcal{A}) for any kernel in the given DNN workload (\mathcal{W}) on the target HULP. Firstly, MEDEA performs *PE Assignment*, selecting the specific PE $p_j \in \mathcal{P}$ for the execution of each kernel k_i . This decision leverages the platform's heterogeneity by matching kernel characteristics to PE strengths. Secondly, for each kernel k_i on the assigned PE, MEDEA determines the efficient *V-F Setting* (v_l, f_l) from the set S_{vf} , enabling kernel-level DVFS.

Thirdly, MEDEA chooses the *Tiling Mode*, critical for managing limited local PE memory (C_{LM_j}) and adhering to kernel-PE operational constraints (λ_{p_j, τ_i} from Λ_{op}). Typically, for the execution of k_i on a PE p_j , operands are transferred

from a shared memory tier (e.g., L2 cache) to p_j 's Local Memory (LM). This movement often necessitates *tiling* when a kernel's data requirements exceed either the LM capacity or other kernel-PE operational limits. Tiling decomposes k_i into smaller, manageable chunks (tiles) whose data footprint adheres to both C_{LM_j} and specific constraints λ_{p_j, τ_i} .

when implementing tiling, MEDEA's role is to decide how to overlap data movement with computation efficiently. It considers two tiling modes, *Single-Buffer Tiling* (t_{sb}) and *Double-Buffer Tiling* (t_{db}). t_{db} aims to hide data movement latency by overlapping the computation of the current tile with the data transfer of the next/previous tile, typically using roughly half of C_{LM_j} for computation buffers. In contrast, t_{sb} maximizes the tile size based on constraints ($C_{LM_j}, \lambda_{p_j, \tau_i}$). Consequently, it has zero overlap between data movement and computation, processing tiles sequentially. MEDEA selects the most efficient mode for each kernel on its assigned PE.

3.3 MEDEA Management and Optimization Algorithm

The primary objective of MEDEA is to generate a schedule that minimizes the total energy consumption, E_t , for executing a given DNN-based application workload \mathcal{W} (defined in Eq. (1)) within a specified timing constraint, deadline T_d . This total energy, E_t , comprises the energy consumed during active DNN execution, $E_{t,a}$, and the energy consumed during any subsequent idle/sleep period, $E_{t,s}$, until the next operational cycle.

$$E_t = E_{t,a} + E_{t,s}. \quad (6)$$

Taking into account idle power P_{slp} and active execution time $T_{t,a} (\leq T_d)$, the total energy to be minimized is:

$$E_t = E_{t,a} + P_{slp} \times \max(0, T_d - T_{t,a}). \quad (7)$$

Timing and Power. To make its decisions, MEDEA leverages characterized timing (S_c) and power (S_p) information. A timing model, $\mathcal{G}_T(\cdot)$, is employed to estimate execution times. This model utilizes measured cycle counts (S_c) for computation, which are obtained for each kernel k_i on a specific PE p_j . The model first estimates the total cycle count for a given kernel and a chosen tiling mode $t_m \in \{t_{sb}, t_{db}\}$. It includes both directly profiled processing-only cycles, extrapolated values for non-profiled kernel sizes, as well as data movement cycles determined by the chosen tiling mode (t_m) and platform constraints (C_{LM_j}, Λ_{op}). Subsequently, this total cycle count is converted to actual execution time by dividing by the operational frequency f_l , which is derived from the selected voltage level v_l and the platform's frequency-voltage mapping S_{vf} . Thus, $\mathcal{G}_T(\cdot)$ provides the estimated execution time of a kernel k_i on a specific PE p_j at a voltage level v_l and using a tiling mode t_m . For power, the model directly uses the characterized power profiles (S_p). It is assumed that the power consumption for a given kernel type τ_i on PE p_j at voltage v_l is independent of the kernel's operational size s_i .

Kernel Execution Configurations. The total active energy, $E_{t,a}$, is the sum of the energies consumed by individual kernels $k_i \in \mathcal{W}$. For each kernel k_i , MEDEA controls several knobs: the PE assignment $p_i \in \mathcal{P}$, the voltage v_i (which determines f_i from S_{vf}), and the execution/tiling mode $c_i \in \{t_{sb}, t_{db}\}$ (as detailed in Section 3.2). A specific combination of these choices for kernel k_i forms an execution configuration, denoted as $\omega_{ij} = (p_{ij}, v_{ij}, c_{ij})$, where j is an index over the possible valid configurations for kernel i . Let Ω_i be the set of all such valid configurations for kernel k_i . A configuration is deemed valid if its execution time $\mathcal{G}_T(\omega_{ij})$ can be successfully estimated (e.g., it is not an invalid mapping due to the PE capability or constraints). The active time and active energy for kernel k_i executed with a

configuration ω_{ij} are:

$$T_a(\omega_{ij}) = \mathcal{G}_T(\omega_{ij}), \quad (8)$$

$$E_a(\omega_{ij}) = \mathcal{G}_P(\omega_{ij}) \times T_a(\omega_{ij}). \quad (9)$$

Optimization Objective Rationale. The overall goal is to minimize the total energy E_t (Eq. (7)) while ensuring the total active time $T_{t,a}$ respects the deadline T_d . This comprehensive objective can be simplified. Consider any valid schedule that meets the deadline with an active time $T_{t,a}$ and active energy $E_{t,a}$. Any alternative schedule that executes faster ($T'_{t,a} < T_{t,a}$) would necessarily require higher V-F settings for some kernels, resulting in a higher active energy consumption ($E'_{t,a} > E_{t,a}$). Furthermore, if the idle power P_{slp} is greater than zero, this faster schedule would also incur a longer subsequent idle period ($T_d - T'_{t,a}$), leading to a higher idle energy consumption ($E'_{t,s} > E_{t,s}$). Since executing faster increases both the active and (for $P_{slp} > 0$) idle energy components, there is no benefit to finishing earlier than necessary. The optimal strategy is therefore to find the schedule that utilizes the available time up to the deadline T_d with the lowest possible active energy. Consequently, the optimization problem simplifies to minimizing the total active energy $E_{t,a}$ subject to the constraint $T_{t,a} \leq T_d$.

Optimization Formulation and Solution. The optimization problem involves selecting one configuration ω_{ij} from Ω_i for each kernel k_i . Before generating the full set Ω_i , for each kernel k_i and each potential PE and V-F pair (p_{ij}, v_{ij}) , MEDEA, utilizing $\mathcal{G}_T(\cdot)$, pre-selects the execution mode c_{ij} (from $\{t_{sb}, t_{db}\}$) that yields the minimum execution cycles (and thus minimum $T_a(\omega_{ij})$ for that (p_{ij}, v_{ij})). This step effectively reduces the dimensionality of the choices before the main optimization. We also define binary decision variables x_{ij} , where $x_{ij} = 1$ if the j -th configuration $\omega_{ij} \in \Omega_i$ is selected for kernel k_i , and 0 otherwise. The optimization problem is to *minimize* total active energy $E_{t,a}$:

$$E_{t,a} = \sum_{i=1}^{N_W} \sum_{\omega_{ij} \in \Omega_i} E_a(\omega_{ij}) \times x_{ij} \quad (10)$$

Subject to:

(1) *Timing Constraint:* Let $T_{t,a} = \sum_{i=1}^{N_W} \sum_{\omega_{ij} \in \Omega_i} T_a(\omega_{ij}) \times x_{ij}$. Then,

$$T_{t,a} \leq T_d \quad (11)$$

(2) *Unique Assignment:* Each kernel must be assigned exactly one configuration:

$$\sum_{\omega_{ij} \in \Omega_i} x_{ij} = 1 \quad \forall i \in \{1, \dots, N_W\} \quad (12)$$

(3) *Binary Decision:* Decision variables are binary:

$$x_{ij} \in \{0, 1\} \quad \forall i \in \{1, \dots, N_W\}, \forall \omega_{ij} \in \Omega_i \quad (13)$$

This optimization problem is then assigned and solved as a Multiple Choice Knapsack Problem (MCKP). In this mapping, each kernel k_i corresponds to an item group, and its valid configurations $\omega_{ij} \in \Omega_i$ represent the items to choose from within that group. The active energy $E_a(\omega_{ij})$ (Eq. (9)) is the *value* or cost associated with selecting item ω_{ij} (to be minimized), its execution time $T_a(\omega_{ij})$ (Eq. (8)) is its *weight*, and the application deadline T_d serves as the knapsack's *capacity*. MEDEA solves this MCKP formulation using an Integer Linear Programming (ILP) solver, such as the one provided by the PuLP library in Python.

Schedule Extraction. The ILP solver yields the optimal set of x_{ij} values. MEDEA then extracts the chosen configuration ω_i^* (which encapsulates the selected p_i^* , v_i^* , and pre-optimized c_i^*) for each kernel k_j for which $x_{ij} = 1$. This sequence of configurations, $\mathcal{A} = \{\omega_1^*, \omega_2^*, \dots, \omega_{N_w}^*\}$, constitutes the final, kernel-level, energy-efficient schedule generated by the manager. The overall MEDEA scheduling process is depicted in Figure 2.

4 Experimental Setup

This section details the experimental methodology for evaluating MEDEA. It covers the evaluation platform including its architecture, implementation, and characterization; the software toolchain; the application case study with its experimental conditions; and the baseline approaches used for comparison.

4.1 Evaluation Platform: HEEPTimize

To evaluate MEDEA in a HULP environment, we use the X-HEEP platform [30], which is a configurable and extensible open source platform designed specifically for accelerator prototyping for edgeAI applications. We use its eXtensible Accelerator InterFace (XAIF) to integrate the accelerators tested with MEDEA. We name the resulting prototyping platform, which has been synthesized for prototyping on a Xilinx Zynq UScale+ FPGA and for power characterization using an ASIC flow, *HEEPTimize* (Figure 3).

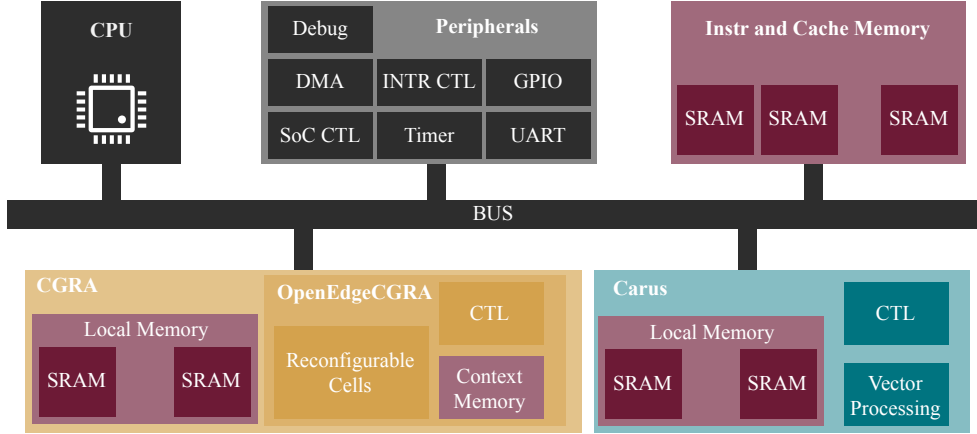


Fig. 3. High-level block diagram of HEEPTimize.

4.1.1 Architecture. HEEPTimize integrates a low-power RISC-V processor with two types of specialized accelerators: an CGRA and an NMC. These three PEs correspond to the set \mathcal{P} , Eq. (2), considered by MEDEA. This selection stems from their demonstrated potential for high energy efficiency and computational flexibility in ULP applications [4, 27]. The main controller is the CV32E40P [29], an open-source, 32-bit, 4-stage, in-order RISC-V core (RV32IMC ISA) optimized for low power. It handles general-purpose tasks, orchestrates accelerator operations, and executes kernels that are not efficiently supported by the specialized units. While OpenEdgeCGRA and Carus excel at some common arithmetically

intensive DNN kernels (e.g., `matmul`, `conv2d`, `add`, `norm`), they are less optimized for complex nonlinear functions or floating-point arithmetic. Consequently, operations such as Softmax, the standard GeLU activation, and floating-point calculations like the logarithm of an FFT’s amplitude are typically offloaded to the host CPU, motivating the hardware-aware model optimizations detailed in Section 4.3. The first accelerator is OpenEdgeCGRA [27], a flexible CGRA. Its architecture comprises a four-by-four mesh of identical reconfigurable cells (RCs) in a torus topology, each equipped with a 32-bit ALU, registers, and private program memory. These RCs operate in a time-multiplexed fashion based on column program counters. Via XAIF, OpenEdgeCGRA utilizes four 32-bit master ports for data memory access and two 32-bit slave ports for its configuration and instruction memory. The second accelerator is Carus [4], an NMC unit optimized for vector operations. It integrates a programmable RISC-V eCPU controller with a scalable Vector Processing Unit (VPU), executing custom `xvnm` ISA vector operations directly on its Vector Register File (VRF), configured with four SRAM banks. The eCPU manages VPU operations using kernel code loaded by the host into a dedicated eMEM, and Carus natively supports 8-bit, 16-bit, and 32-bit fixed-point data. Reflecting its NMC design, Carus connects via a single XAIF slave port for eMEM programming and control, which lacks external master ports. The completion of the computation for both OpenEdgeCGRA and Carus is signaled to the host CPU via XAIF-routed interrupt lines to the interrupt controller.

The memory hierarchy is designed to support these PEs. Carus operates on its internal 64 KiB LM (or VRF). For operational similarity and fair comparison, OpenEdgeCGRA is provided with a dedicated 64 KiB LM. These LM capacities correspond to C_{LM_j} values in C_{LM} (Eq. (4)). A shared 128 KiB L2 cache acts as an intermediate data buffer between these accelerator LMs and the off-chip NAND flash memory, where application data such as model parameters are stored. DMA controllers manage data transfers between flash and the L2 cache, and subsequently between the L2 cache and the respective accelerator LMs. This L2 cache also facilitates double buffering techniques during processing.

4.1.2 Implementation and Characterization. Characterization of HEEPTimize, in the absence of fabricated silicon, was based on a combination of FPGA prototyping for timing validation and an ASIC implementation flow for power and area analysis. While FPGA prototyping yields accurate cycle counts for kernel execution, precise power estimation requires simulation using industry-standard Electronic Design Automation (EDA) tools.

FPGA Prototyping. To facilitate functional verification and obtain realistic kernel execution cycle counts, the HEEPTimize architecture was implemented and prototyped on a Xilinx ZCU104 Ultrascale+ FPGA development board. The cycle counts measured from the execution of representative DNN kernels on each PE on the FPGA serve as input for the timing profiles used by MEDEA (as detailed in Section 3.1.3).

ASIC Implementation (GF 22 nm FDX). For accurate power and area analysis, HEEPTimize was designed using a standard cell ASIC flow targeting the GlobalFoundries (GF) 22 nm Fully Depleted Silicon-on-Insulator (FDX) technology node, chosen for its suitability for low-power applications. Logic synthesis for the entire design was performed using Synopsys Design Compiler (DC), targeting the worst-case Slow-Slow Global (SSG) process corner to ensure robust timing closure across process variations. On-chip memories (L2 cache, instruction memory, and local memories) were generated using the GF 22 nm FDX S1DU SRAM compiler, selected for its ULP characteristics.

Timing Analysis (Max Frequency). Static Timing Analysis (STA), performed using Synopsys PrimePower, determined the maximum operating frequency (f_{max}) achievable at each supported voltage level (0.5 V, 0.65 V, 0.8 V, and 0.9 V). These characterized maximum frequencies form the basis of the S_{of} set (Eq. (3)) and are crucial for the DVFS model in MEDEA. The results are presented in Table 2.

Table 2. HEEPTimize Maximum Operating Frequencies vs. Voltage (GF 22 nm FDX)

Voltage (V)	0.50	0.65	0.80	0.90
Max Freq. (MHz)	122	347	578	690

Power Analysis. System-level post-synthesis simulations were performed using Siemens QuestaSim on the synthesized netlist to capture realistic operational behavior during the execution of representative DNN kernels. Detailed switching activity information from these simulations was logged into Value Change Dump (VCD) files. The synthesized netlist and the generated VCD files were then input into Synopsys PrimePower for dynamic power analysis, conducted under typical-typical (TT) operating conditions. This tool calculates power consumption based on the standard cell library’s power models and the captured switching activity, providing a breakdown into Static (Leakage) Power (P_{stat}) and Dynamic Power (P_{dyn_b} at the simulation frequency, f_b). To obtain power profiles across different voltages ($v_l \in \mathcal{V}$), this analysis was repeated using standard cell libraries characterized for each supported voltage level (0.5 V, 0.65 V, 0.8 V, and 0.9 V).

Area Results. The breakdown of the post-synthesis area for HEEPTimize, which details the contribution of various parts of the memory, processor and accelerators, and peripherals, was obtained after synthesis with Synopsys DC (SSG corner), is reported in Table 3.

Table 3. Post-Synthesis Area Breakdown of HEEPTimize (GF 22 nm FDX, SSG Corner)

Component	Area (mm ²)
CPU Subsystem	0.021
Carus (NMC, incl. 64 KiB VRF)	0.110
OpenEdgeCGRA (Logic)	0.085
CGRA Local Memory (64 KiB)	0.091
L2 Cache (128 KiB)	0.181
Instruction Memory (64 KiB)	0.091
Peripherals	0.053
Total Area	≈0.632

4.2 Software Toolchain and Compilation

All software components, including DNN kernels executed on the CPU and accelerator control code, were compiled using the *GNU RISC-V GCC compiler, version 11.1.0* applying the `-O2` optimization level. Kernels targeted for the main RISC-V CPU (CV32E40PX) were compiled for the standard RV32IMC instruction set. Kernels designated for the NMC accelerator (Carus) were developed in C and RISC-V assembly, leveraging the custom `xvnmc` vector ISA extension. These were compiled using an extended version of the GNU RISC-V GCC toolchain incorporating assembler support for `xvnmc` and loaded into Carus’s local instruction memory (eMEM) by the host CPU at runtime.

4.3 Application Case Study and Experimental Condition

TSD Model Description. We evaluated MEDEA using the *Transformer for Seizure Detection (TSD)* model [1, 21]. This model was chosen for its relevance to ULP biomedical applications and exemplifies the trend of employing transformer

architectures for complex signal processing tasks on these platforms. The TSD model is based on a Vision Transformer (ViT) architecture specifically designed for epileptic seizure detection using EEG data. It comprises four transformer encoder blocks, each containing a multi-head self-attention (MHSA) layer and a feed-forward network (FFN). Figure 4 shows the detailed model architecture, illustrating its decomposition into processing kernels. The model was trained and tested using the publicly available Temple University Hospital EEG Seizure Corpus (TUSZ)-v2.0.0 [21].

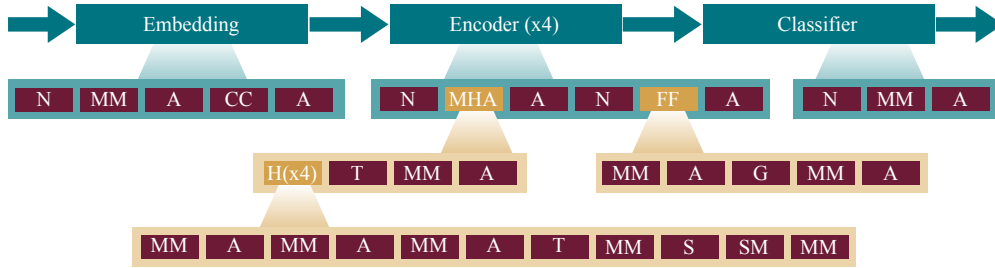


Fig. 4. TSD model architecture, illustrating the decomposition into processing kernels (where G=GeLU, SM=SoftMax, T=Transpose, S=Scale, N=Norm, MM=MatMul, A=Add, CC=ClassConcat, MHA=Multi-Head Attention, FF=FeedForward, and H=Head).

TSD Model Modifications. The kernels that were not compatible with the HEEPTimize’s accelerators were optimized in SW using reasonable effort to facilitate that the application can be executed in an ULP.

Key modifications include: replacing the original floating-point Softmax layer with a *constant Softmax* approximation using a 3-coefficient Taylor expansion (following the approach in [18]); direct use of the *magnitude of the fast Fourier transform (FFT)* results instead of the logarithm of the FFT amplitude used in the original work [1, 21]; and implementation of the GeLU activation function via a *piecewise linear (PWL) approximation*, replacing its standard floating-point computation. These modifications significantly reduce computational complexity, particularly for components not easily accelerated on HEEPTimize’s specialized hardware, making the original application more suitable for execution on ULP devices. As shown in Table 4, the CPU cycle counts for these specific operations were drastically reduced. While retraining showed minimal impact on the F1-score for the Softmax and GeLU changes (66.0 % vs. 66.6 %), using the FFT magnitude instead of log-amplitude resulted in a final F1-score of 60.3 %, deemed an acceptable exchange for the significant reduction of 98 % achieved in execution cycles on these kernels.

Table 4. CPU Cycles Reduction from TSD Model Modifications

Operation	Original Cycles (M)	Modified Cycles (M)
Log-Amplitude FFT	~182	~11.00
Softmax	~647	~5.00
GeLU	~8	~0.03

Experimental Conditions. To comprehensively evaluate MEDEA’s adaptability and performance, particularly for applications with stringent or varying real-time demands such as continuous inference in biomedical scenarios, the TSD model (specifically its transformer core for most comparative analyses) is evaluated under three distinct timing constraints (T_d): 50 ms (stringent), 200 ms (moderate), and 1000 ms (relaxed). These varying deadlines allow us to assess how MEDEA manages the energy-performance tradeoff when dealing with different application timing requirements.

4.4 Comparison Baselines

To quantify the benefits of MEDEA, its performance is compared against several baseline scheduling and management strategies adapted from principles observed in the literature. A necessary step for evaluation on memory-constrained platforms like HEEPTimize was the incorporation of memory management. As many related works (e.g., [2, 12, 23]) do not inherently include the required memory-aware tiling, we consistently applied tiling using the double buffering (t_{db}) strategy (Section 3.2) across all evaluated methods, ensuring feasibility and comparability on our hardware. We evaluate and compare against the following baselines, representing increasing levels of optimization sophistication:

- CPU (MaxVF): A non-DVFS, homogeneous approach running the workload entirely on the CPU at its maximum V-F setting.
- StaticAccel (MaxVF): selects a priori the single most energy-efficient accelerator for the TSD workload and runs it at maximum V-F, offloading unsupported kernels to the CPU; this is conceptually similar to static accelerator selection in works like [35, 36].
- StaticAccel (AppDVFS): Applies application-level DVFS to the StaticAccel (MaxVF) configuration by selecting a single optimal V-F setting for the entire execution of the chosen accelerator, similar to strategies proposed in [13, 17, 23].
- CoarseGrain (AppDVFS): Represents approaches that schedule larger functional blocks by selecting the most energy-efficient PE for predefined *groups* of kernels and applying a single application-level DVFS setting. For the TSD model, we define these groups based on the logical components of the transformer architecture: The initial input embedding forms one group; within each encoder layer, the normalization, each multi-head attention head, the feed-forward network, and the residual connection are each treated as separate groups; and a final group is formed for the classification block. This grouping strategy reflects works that schedule larger blocks (e.g., [2]) while incorporating basic energy-aware PE selection (conceptually similar to [9, 26]).

5 Results and Analysis

This section presents the experimental results, conducted on HEEPTimize (Section 4.1). We first analyze MEDEA’s performance for running TSD model under varying timing constraints (Section 4.3) and compare it against the defined baselines (Section 4.4), and then examine its adaptive scheduling decisions. Subsequently, we dissect the contributions of isolated MEDEA’s key features to its overall energy efficiency.

5.1 MEDEA Performance Evaluation

Figure 5 presents the total energy consumption (E_t) and active execution time ($T_{t,a}$) for the inference decisions generated by MEDEA and the evaluated baselines (Section 4.4) across the three defined timing constraints for the TSD transformer core. Note that E_t for each scenario in Figure 5 represents the energy consumed over one complete inference window, with the duration of this window being defined by its corresponding deadline (T_d). Table 5 further details the energy and time breakdown specifically for MEDEA’s decisions, highlighting the interplay between active and idle components. With relaxed timing constraints (e.g., $T_d = 1000$ ms), a significant portion of the deadline window is spent idle ($T_{t,s}$), making idle energy ($E_{t,s}$) prominent. This underscores the importance of platform idle power (P_{slp}), especially when timing constraints are not demanding, as also noted in [33].

As depicted in Figure 5, executing the TSD model solely on the CPU consumes excessive energy and fails to meet the 50 ms deadline, confirming the need for hardware acceleration. The *StaticAccel* baseline, while meeting deadlines, incurs

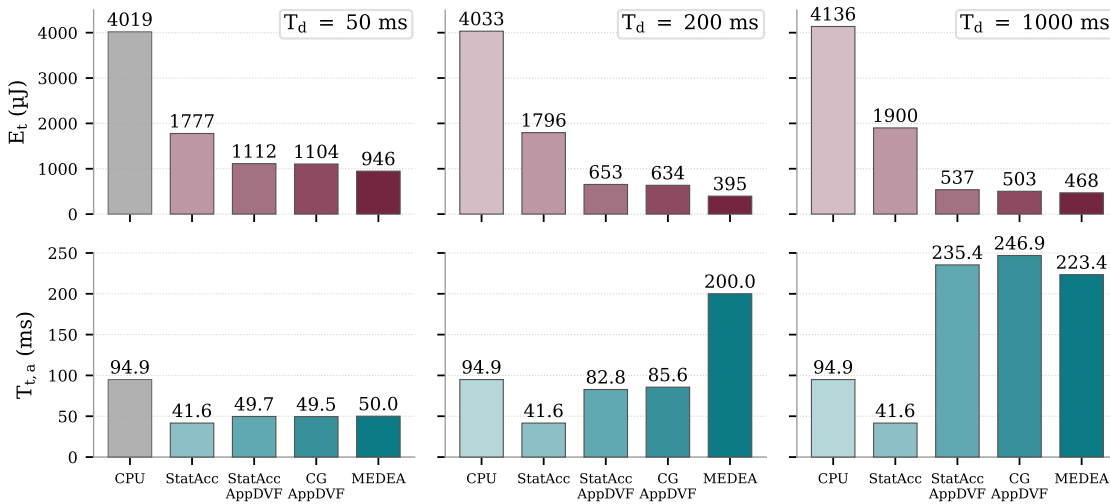


Fig. 5. Total energy and active execution time of one window while running the TSD model using MEDEA versus baseline schedulers under timing constraints of 50 ms, 200 ms, and 1000 ms.

Table 5. End-to-End Time and Energy Breakdown for the TSD workload using MEDEA (Sleep power $P_{slp} = 129 \mu\text{W}$).

Deadline (ms)	Active Time (ms)	Sleep Time (ms)	Active Energy (μJ)	Sleep Energy (μJ)
50	50	0	946	0
200	200	0	395	0
1000	223	777	368	100

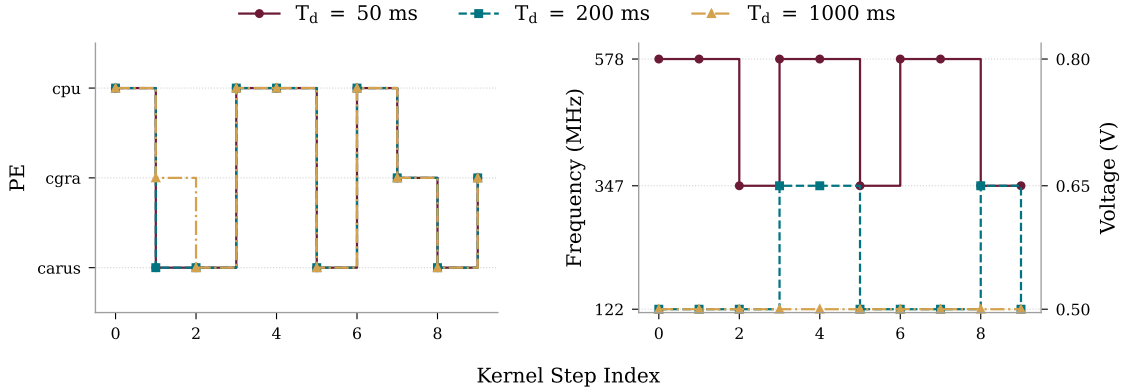
high energy costs due to its lack of DVFS and inflexibility in leveraging platform heterogeneity. Introducing application-level DVFS via *StaticAccel-AppDVF* reduces energy compared to the non-DVFS version but still underutilizes platform heterogeneity. Leveraging heterogeneity with *CoarseGrain(CG)-AppDVF*, while an improvement over single-accelerator strategies, sees its efficiency limited by coarse granularity, a simple DVFS scheme, and the absence of explicit timing constraint-based optimization during its PE selection and AppDVFS determination.

In contrast, MEDEA consistently optimizes energy consumption to achieve an energy-efficient solution while meeting the deadline across all evaluated scenarios. For instance, when compared to the *CoarseGrain (AppDVFS)* baseline, MEDEA achieves energy savings of approximately 14% for the 50 ms deadline, 38% for the 200 ms deadline, and 7% for the 1000 ms deadline, always outperforming the baselines while successfully meeting all timing constraints. This superior performance is a direct result of the integrated features of MEDEA.

5.2 MEDEA Optimized Decisions

As established in Section 3.3, MEDEA achieves the energy savings demonstrated above by solving an optimization problem that seeks to minimize active energy ($E_{t,a}$) under the given timing constraint (T_d). The core decisions from this optimization involve selecting the PE and V-F setting for each kernel, with the tiling mode being a pre-determined

choice for each PE-VF pair. To visualize these decisions in action, Figure 6 provides a snapshot of MEDEA’s generated decisions for an illustrative sequence of kernels from the TSD transformer model under the three evaluated timing constraints. The figure clearly illustrates that as the timing constraint becomes more stringent (e.g., tightening from 1000 ms down to 50 ms), MEDEA strategically utilizes higher V-F settings to ensure timeliness, a direct application of kernel-level DVFS. Under the relaxed 1000 ms deadline, MEDEA operates PEs at the lowest available V-F setting (e.g., 0.5 V), as this is sufficient to meet the deadline. In such scenarios where the kernel-level DVFS knob offers limited room for further optimization, the marginal energy improvement becomes less pronounced.



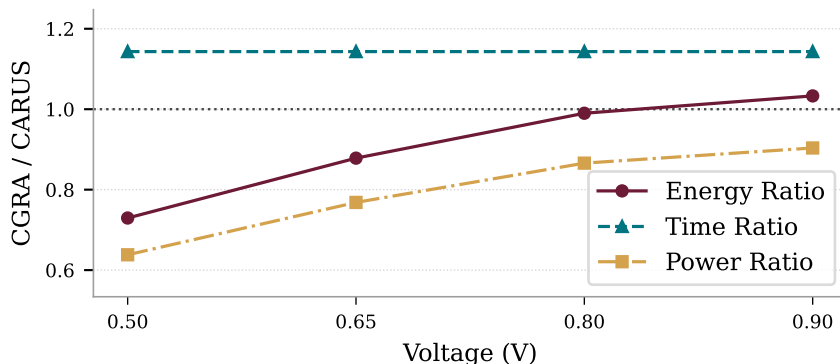


Fig. 7. TSD matmul subset: Ratio of CGRA performance and energy metrics (Energy, Power, Time) over Carus metrics versus V-F setting.

illustrate the potential energy inefficiencies in related works that lack these capabilities. The core features analyzed are: (1) kernel-level runtime DVFS, (2) kernel-level scheduling, and (3) memory-aware adaptive tiling.

Table 6 presents the absolute total energy consumption (E_t) for these configurations in the three timing constraints (T_d) for the TSD model. To better visualize the impact, Figure 8 shows the corresponding percentage energy reduction achieved by each feature. This percentage of savings is calculated as $(E_{w/oFeat} - E_{Full}) / E_{w/oFeat} \times 100$, where $E_{w/oFeat}$ is the energy consumed with that specific feature disabled.

Table 6. Energy consumption (μ J) for MEDEA feature analysis under different timing constraints.

Sched. Setup	Deadline (ms)		
	50	200	1000
Full MEDEA	946	395	468
w/o KerDVFS	1002	576	468
w/o AdapTile	1030	432	492
w/o KerSched	974	404	473

5.3.1 Impact of Kernel-level DVFS. First, we analyze the impact of kernel-level DVFS. We compare the full MEDEA against a configuration where all other features are active, but a single application-level DVFS (AppDVFS) setting is used. This AppDVFS setting is the lowest V-F point that allows the schedule to meet the deadline. Figure 8 shows that enabling kernel-level DVFS (i.e., using AppDVFS) yields no additional energy savings for the 1000 ms deadline. This is expected, as under such a relaxed constraint, MEDEA already uses the lowest V-F setting for all kernels, making kernel-level DVFS adjustments redundant. However, for the 200 ms deadline, enabling kernel-level DVFS provides a significant 31.3 % energy saving. For the 50 ms deadline, the saving is 5.6 %. This demonstrates that kernel-level DVFS is most impactful when the deadline allows for a diverse range of V-F settings across kernels; for very tight deadlines (such as 50 ms), most kernels are forced to higher V-F settings, reducing the scope for differential benefits of DVFS compared to an optimized AppDVFS.

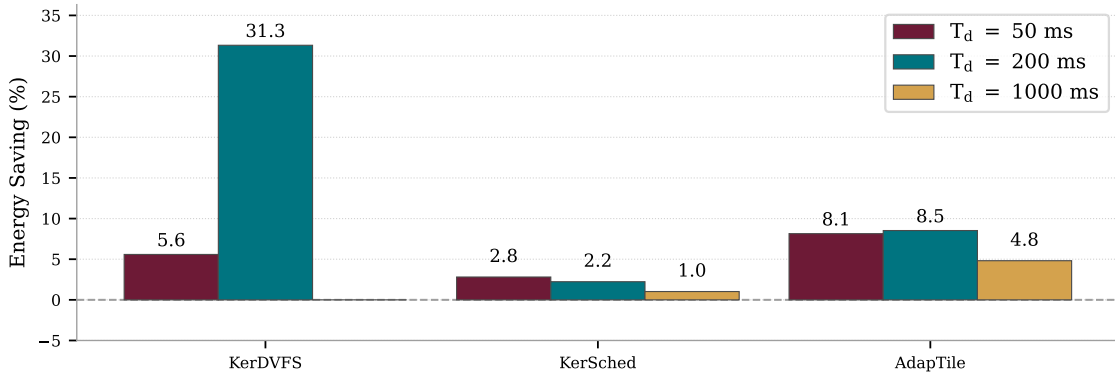


Fig. 8. Energy saving when selectively disabling core MEDEA features for the TSD model under different timing constraints.

5.3.2 Impact of Kernel-level Scheduling. Although kernel-level DVFS and scheduling are intertwined, we isolate the impact of scheduling granularity. Here, we compare the full MEDEA approach against a configuration that uses coarse-grained scheduling (grouping kernels as defined in Section 5.1 for the CoarseGrain-AppDVFS baseline) but still applies group-level DVFS and all other optimizations. As seen in Figure 8, moving to fine-grained, per-kernel scheduling provides an energy saving between 1.0% to 2.8% across the deadlines. Although modest, this indicates that even with per-group DVFS, forcing a single PE/V-F choice for a diverse group of kernels can lead to suboptimal energy assignments for individual kernels within that group compared to per-kernel decision-making.

5.3.3 Impact of Adaptive Tiling. Finally, we assess the contribution of MEDEA’s memory-aware adaptive tiling by comparing it against a configuration with a fixed, non-adaptive tiling strategy (always defaulting to double-buffering, t_{db} , regardless of kernel size or memory pressure) while keeping all other features active. Enabling adaptive tiling, as shown in Figure 8, results in energy savings of 8.1% (50 ms), 8.5% (200 ms), and 4.8% (1000 ms). The consistent savings highlight the importance of dynamically selecting the best tiling mode (t_{sb} vs. t_{db}) based on kernel characteristics to optimize data movement and memory utilization. The slightly lower impact at 1000 ms might be influenced by longer idle times, which could mask smaller differences in active energy due to tiling choices.

6 Conclusion

This paper has addressed the critical challenge of achieving energy-efficient DNN inference on resource-constrained HULPs. We introduced MEDEA, a novel design-time multi-objective manager that uniquely integrates kernel-level scheduling, kernel-level runtime DVFS, and memory-aware adaptive tiling, all driven by a timing-constrained energy optimization strategy. Through a comprehensive evaluation on HEEPTimize, a custom HULP, MEDEA demonstrated its ability to deliver significant energy efficiency, achieving energy reductions of up to 38% compared to the relevant adapted baselines while consistently meeting strict application deadlines. Our in-depth analyses further quantified the significant individual contributions of MEDEA’s core features. Overall, this work has proposed a robust and adaptive manager essential for realizing the full potential of HULP systems for complex AI workloads, paving the way for more sophisticated intelligent applications on severely constrained devices.

Acknowledgments

The authors would like to thank María José Belda for her help in providing the kernels for CGRA, Michele Caon for his help in providing the evaluated DNN kernels for NMC, and Simone Machetti, Davide Schiavone and Luigi Giuffrida for their support on the platform setup part. We thank Jan Tomasz Juraszek for his help during a semester project on verifying that our TSD optimizations maintained acceptable model performance. This research is carried out in the frame of the “UrbanTwin: An urban digital twin for climate action: Assessing policies and solutions for energy, water and infrastructure” project with the financial support of the ETH-Domain Joint Initiative program in the Strategic Area Energy, Climate and Sustainable Environment. Also, this work was supported in part by the Swiss State Secretariat for Education, Research, and Innovation (SERI) through the SwissChips research project.

References

- [1] Alireza Amirshahi, Maedeh H Toosi, Siamak Mohammadi, Stefano Albini, Pasquale Davide Schiavone, Giovanni Ansaloni, Amir Aminifar, and David Atienza. 2024. MetaWearS: A Shortcut in Wearable Systems Lifecycle with Only a Few Shots. *arXiv preprint arXiv:2408.01988* (2024).
- [2] Halima Bouzidi, Mohamad Odema, Hamza Ouarnoughi, Smail Niar, and Mohammad Abdullah Al Faruque. 2023. Map-and-conquer: Energy-efficient mapping of dynamic neural nets onto heterogeneous MPSoCs. In *DAC*. IEEE, 1–6.
- [3] Alessio Burrello, Angelo Garofalo, Nazareno Bruschi, Giuseppe Tagliavini, Davide Rossi, and Francesco Conti. 2021. DORY: Automatic end-to-end deployment of real-world DNNs on low-cost IoT MCUs. *IEEE Trans. Comput.* 70, 8 (2021), 1253–1268.
- [4] Michele Caon, Clément Choné, Pasquale Davide Schiavone, Alexandre Levisse, Guido Masera, Maurizio Martina, and David Atienza. 2025. Scalable and RISC-V Programmable Near-Memory Computing Architectures for Edge Nodes. *IEEE Transactions on Emerging Topics in Computing* (2025).
- [5] Ismet Dagli and Mehmet E Belviranlı. 2024. Shared memory-contention-aware concurrent DNN execution for diversely heterogeneous system-on-chips. In *ACM SIGPLAN Annual Symposium on Principles and Practice of Parallel Programming*. 243–256.
- [6] Ismet Dagli, Alexander Cieslewicz, Jedidiah McClurg, and Mehmet E Belviranlı. 2022. Axonn: Energy-aware execution of neural network inference on multi-accelerator heterogeneous SoCs. In *DAC*. 1069–1074.
- [7] Benoît Walter Denking, Miguel Peón-Quirós, Mario Konijnenburg, David Atienza, and Francky Catthoor. 2023. Acceleration of control intensive applications on coarse-grained reconfigurable arrays for embedded systems. *IEEE Trans. Comput.* 72, 9 (2023), 2548–2560.
- [8] Angelo Garofalo, Yvan Tortorella, Matteo Perotti, Luca Valente, Alessandro Nadalini, Luca Benini, Davide Rossi, and Francesco Conti. 2022. DARKSIDE: A heterogeneous RISC-V compute cluster for extreme-edge on-chip DNN inference and training. *IEEE Open Journal of the Solid-State Circuits Society* 2 (2022), 231–243.
- [9] Mohamed Amine Hamdi, Francesco Daghero, Giuseppe Maria Sarda, Josse Van Delm, Arne Symons, Luca Benini, Marian Verhelst, Daniele Jahier Pagliari, and Alessio Burrello. 2025. MATCH: Model-Aware TVM-based Compilation for Heterogeneous Edge Devices. *IEEE Transactions on Computer-Aided Design of Integrated Circuits and Systems* (2025).
- [10] Eunjin Jeong, Jangryul Kim, Samnieng Tan, Jaeseong Lee, and Soonhoi Ha. 2021. Deep learning inference parallelization on heterogeneous processors with TensorRT. *IEEE Embedded Systems Letters* 14, 1 (2021), 15–18.
- [11] Victor JB Jung, Alessio Burrello, Moritz Scherer, Francesco Conti, and Luca Benini. 2024. Optimizing the deployment of tiny transformers on low-power MCUs. *IEEE Trans. Comput.* (2024).
- [12] Andreas Kosmas Kakolyris, Manolis Katsaragakis, Dimosthenis Masouros, and Dimitrios Soudris. 2023. RoaD-RuNNer: Collaborative DNN partitioning and offloading on heterogeneous edge systems. In *DATE*. IEEE, 1–6.
- [13] Duseok Kang, Jinwoo Oh, Jongwoo Choi, Youngmin Yi, and Soonhoi Ha. 2020. Scheduling of deep learning applications onto heterogeneous processors in an embedded device. *IEEE Access* 8 (2020), 43980–43991.
- [14] Andreas Karatzas and Iraklis Anagnostopoulos. 2023. OmniBoost: Boosting throughput of heterogeneous embedded devices under multi-DNN workload. In *DAC*. IEEE, 1–6.
- [15] Ben Keller, Martin Cochet, Brian Zimmer, Jaehwa Kwak, Alberto Puggelli, Yunsup Lee, Milovan Blagojević, Stevo Bailey, Pi-Feng Chiu, Palmer Dabbelt, et al. 2017. A RISC-V processor SoC with integrated power management at submicrosecond timescales in 28 nm FD-SOI. *IEEE Journal of Solid-State Circuits* 52, 7 (2017), 1863–1875.
- [16] Siqin Liu and Avinash Karanth. 2021. Dynamic voltage and frequency scaling to improve energy-efficiency of hardware accelerators. In *IEEE HiPC*. IEEE, 232–241.
- [17] Sicong Liu, Hao Luo, XiaoChen Li, Yao Li, Bin Guo, Zhiwen Yu, YuZhan Wang, Ke Ma, YaSan Ding, and Yuan Yao. 2024. AdaKnife: Flexible DNN offloading for inference acceleration on heterogeneous mobile devices. *IEEE Transactions on Mobile Computing* (2024).
- [18] Shiwei Liu, Guanchen Tao, Yifei Zou, Derek Chow, Zichen Fan, Kauna Lei, Bangfei Pan, Dennis Sylvester, Gregory Kielian, and Mehdi Saligane. 2024. Consmax: Hardware-friendly alternative softmax with learnable parameters. *arXiv preprint arXiv:2402.10930* (2024).

- [19] Simone Machetti, Pasquale Davide Schiavone, Christoph Thomas Müller, Alexandre Sébastien Julien Levisse, Miguel Peón-Quirós, and David Atienza. 2024. HEEPocrates: An ultra-low-power RISC-V microcontroller for edge-computing healthcare applications. (2024).
- [20] Simone Machetti, Pasquale Davide Schiavone, Thomas Christoph Müller, Miguel Peón-Quirós, and David Atienza. 2024. X-HEEP: An open-source, configurable and extendible RISC-V microcontroller for the exploration of ultra-low-power edge accelerators. *arXiv preprint arXiv:2401.05548* (2024).
- [21] Taraneh Aminosharieh Najafi, Jose Miranda, Jérôme Thevenot, Benjamin Duc, Stefano Albini, Alireza Amirshahi, Hossein Taji, Maria José Belda, Antonio Affanni, and David Atienza. 2024. VersaSens: An Extendable Multimodal Platform for Next-Generation Edge-AI Wearables. *IEEE Transactions on Circuits and Systems for Artificial Intelligence* (2024).
- [22] Ricardo Núñez-Prieto, David Castells-Rufas, and Lluís Terés-Terés. 2023. RisCO2: Implementation and Performance Evaluation of RISC-V Processors for Low-Power CO2 Concentration Sensing. *Micromachines* 14, 7 (2023), 1371.
- [23] Mohanad Odema, Halima Bouzidi, Hamza Ouarnoughi, Smail Niar, and Mohammad Abdullah Al Faruque. 2023. Magnas: A mapping-aware graph neural architecture search framework for heterogeneous MPSoC deployment. *ACM Transactions on Embedded Computing Systems* 22, 5s (2023), 1–26.
- [24] Flavio Ponzina, Simone Machetti, Marco Rios, Benoît Walter Denking, Alexandre Levisse, Giovanni Ansaloni, Miguel Peón-Quirós, and David Atienza. 2022. A hardware/software co-design vision for deep learning at the edge. *IEEE Micro* 42, 6 (2022), 48–54.
- [25] Partha Pratim Ray. 2022. A review on TinyML: State-of-the-art and prospects. *Journal of King Saud University-Computer and Information Sciences* 34, 4 (2022), 1595–1623.
- [26] Matteo Rizzo, Alessio Burrello, and Daniele Jahier Pagliari. 2025. Optimizing DNN Inference on Multi-Accelerator SoCs at Training-time. *IEEE Transactions on Computer-Aided Design of Integrated Circuits and Systems* (2025).
- [27] Rubén Rodríguez Álvarez, Benoît Denking, Juan Sapriza, José Miranda, Giovanni Ansaloni, and David Atienza. 2023. An open-hardware coarse-grained reconfigurable array for edge computing. In *ACM International Conference on Computing Frontiers*. 391–392.
- [28] Moritz Scherer. 2024. *Hardware-Software Co-Design for Energy-Efficient Neural Network Inference at the Extreme Edge*. Ph.D. Dissertation. ETH Zurich.
- [29] Pasquale Davide Schiavone, Francesco Conti, Davide Rossi, Michael Gautschi, Antonio Pullini, Eric Flamand, and Luca Benini. 2017. Slow and steady wins the race? A comparison of ultra-low-power RISC-V cores for Internet-of-Things applications. In *PATMOS*. IEEE, 1–8.
- [30] Pasquale Davide Schiavone, Simone Machetti, Miguel Peón-Quirós, Jose Miranda, Benoît Denking, Thomas Christoph Müller, Rubén Rodríguez Álvarez, Saverio Nasturzio, and David Atienza. 2023. X-HEEP: An Open-Source, Configurable and Extendible RISC-V Microcontroller. In *ACM International Conference on Computing Frontiers*. 379–380.
- [31] Nikolaos Schizas, Aristeidis Karras, Christos Karras, and Spyros Sioutas. 2022. TinyML for ultra-low power AI and large scale IoT deployments: A systematic review. *Future Internet* 14, 12 (2022), 363.
- [32] Rafael Stahl, Daniel Mueller-Gritschneider, and Ulf Schlichtmann. 2023. Fused depthwise tiling for memory optimization in tinyML deep neural network inference. *arXiv preprint arXiv:2303.17878* (2023).
- [33] Hossein Taji, José Miranda, Miguel Peón-Quirós, and David Atienza. 2024. Energy-Efficient Frequency Selection Method for Bio-Signal Acquisition in AI/ML Wearables. In *ACM/IEEE ISLPED*. 1–6.
- [34] Kodai Ueyoshi, Ioannis A Papistas, Pouya Houshmand, Giuseppe M Sarda, Vikram Jain, Man Shi, Qilin Zheng, Sebastian Giraldo, Peter Vranx, Jonas Dovenspeck, et al. 2022. DIANA: An end-to-end energy-efficient digital and ANALog hybrid neural network SoC. In *ISSCC*, Vol. 65. IEEE, 1–3.
- [35] Giorgos Vasiliadis, Rafail Tsirbas, and Sotiris Ioannidis. 2022. The best of many worlds: Scheduling machine learning inference on CPU-GPU integrated architectures. In *IEEE IPDPSW*. IEEE, 55–64.
- [36] Siqi Wang, Anuj Pathania, and Tulika Mitra. 2020. Neural network inference on mobile SoCs. *IEEE Design & Test* 37, 5 (2020), 50–57.
- [37] Yecheng Xiang and Hyoseung Kim. 2019. Pipelined data-parallel CPU/GPU scheduling for multi-DNN real-time inference. In *IEEE RTSS*. IEEE, 392–405.
- [38] Josip Zidar, Tomislav Matić, Ivan Aleks, and Željko Hocenski. 2024. Dynamic voltage and frequency scaling as a method for reducing energy consumption in ultra-low-power embedded systems. *Electronics* 13, 5 (2024), 826.